nature neuroscience

Presynaptic regulation of quantal size: K^+/H^+ exchange stimulates vesicular glutamate transport

Germaine Y Goh[1], Hai Huang[2,4], Julie Ullman[1,3,4], Lars Borre[1], Thomas S Hnasko[1], Laurence O Trussell[2] & Robert H Edwards[1]

The amount of neurotransmitter stored in a single synaptic vesicle can determine the size of the postsynaptic response, but the factors that regulate vesicle filling are poorly understood. A proton electrochemical gradient ($\Delta\mu_{H+}$) generated by the vacuolar H^+-ATPase drives the accumulation of classical transmitters into synaptic vesicles. The chemical component of $\Delta\mu_{H+}$ (ΔpH) has received particular attention for its role in the vesicular transport of cationic transmitters as well as in protein sorting and degradation. Thus, considerable work has addressed the factors that promote ΔpH. However, synaptic vesicle uptake of the principal excitatory transmitter glutamate depends on the electrical component of $\Delta\mu_{H+}$ (Δψ). We found that rat brain synaptic vesicles express monovalent cation/H^+ exchange activity that converts ΔpH into Δψ, and that this promotes synaptic vesicle filling with glutamate. Manipulating presynaptic K^+ at a glutamatergic synapse influenced quantal size, indicating that synaptic vesicle K^+/H^+ exchange regulates glutamate release and synaptic transmission.

It is known that the response to release of neurotransmitter from a single synaptic vesicle (quantal size) can vary as a result of postsynaptic changes in receptors[1], but considerably less is known about the presynaptic regulation of quantal size through changes in vesicle filling with transmitter. Glutamate receptors are not saturated at the calyx of Held[2,3] and synapses in the hippocampus and cerebellum[4,5], indicating that changes in the amount of glutamate released per synaptic vesicle have the potential to influence miniature excitatory postsynaptic current (mEPSC) amplitude. Indeed, synaptic vesicle enlargement resulting from alterations in endocytosis can increase quantal size[6,7].

Previous work has suggested that changes in the expression of vesicular glutamate transporters (VGLUTs) may affect vesicle filling. Neural activity has been shown to regulate the expression of VGLUT mRNA[8], and decreased expression reduces quantal size in cultures from knockout mice[9]. Heterozygous animals also have physiological and behavioral defects[10,11]. However, we previously observed no difference in quantal size between VGLUT1 heterozygotes and wild-type animals at hippocampal synapses[12]. Furthermore, a single VGLUT protein suffices to fill one synaptic vesicle in *Drosophila*[13], suggesting that VGLUT expression may influence the rate of vesicle filling rather than the gradient of transmitter achieved at equilibrium. However, changes in transport activity (rather than simply expression) have generally received little attention[14].

The transport of all classical transmitters into synaptic vesicles depends on a H^+ electrochemical gradient ($\Delta\mu_{H+}$) across the vesicle membrane. Generated by the vacuolar H^+-translocating ATPase (V-ATPase), $\Delta\mu_{H+}$ comprises both a chemical gradient (ΔpH) and membrane potential (Δψ)[15]. The relative roles of ΔpH and Δψ in turn vary with the stoichiometry of ionic coupling by different vesicular neurotransmitter transporters. Vesicular monoamine and acetylcholine transporters exchange two lumenal protons for one cationic transmitter, resulting in a greater dependence on ΔpH than Δψ[16–18]. However, the V-ATPase initially produces Δψ, which arrests its activity and prevents it from making ΔpH. The production of ΔpH therefore requires the entry of an anion such as Cl^- to dissipate Δψ, thereby activating the V-ATPase[19–22].

Although the stoichiometry of ionic coupling by the VGLUTs remains unknown, with the role of H^+ unclear, these carriers rely more on Δψ than ΔpH[20,21]. As a result, glutamate entry acidifies synaptic vesicles[20,23,24], limiting the ability of the H^+ pump to create the Δψ required for VGLUT activity. Despite the importance of Δψ for vesicular glutamate transport, however, little is known about the mechanisms that promote its formation or its role in the secretory pathway.

RESULTS

Synaptic vesicles exhibit electroneutral cation/H^+ exchange

A number of possible mechanisms might serve to dissipate the ΔpH accumulated during vesicular glutamate transport and thus increase the production of Δψ by the V-ATPase. First, a H^+ leak might simply allow the efflux of protons down their electrochemical gradient, but this would reduce Δψ as well as ΔpH[19]. Second, the efflux of anions from synaptic vesicles might itself create positive Δψ, independent of the H^+ pump. This would require an outwardly directed anion gradient, and recent work using VGLUT1 reconstituted into artificial membranes found that chloride efflux can promote vesicular glutamate transport[25], although its physiological importance remains unknown. Alternatively, the influx of cytoplasmic cation might increase Δψ by

[1]Departments of Physiology and Neurology, Graduate Programs in Neuroscience, Cell Biology and Bioengineering, University of California, San Francisco, San Francisco, California, USA. [2]Oregon Hearing Research Center and Vollum Institute, Oregon Health and Science University, Portland, Oregon, USA. [3]Graduate Program in Molecular and Cellular Biology, University of California, Berkeley, Berkeley, California, USA. [4]These authors contributed equally to this work. Correspondence should be addressed to R.H.E. (robert.edwards@ucsf.edu).

Received 23 May; accepted 11 July; published online 28 August 2011; corrected online 13 October 2011 (details online); doi:10.1038/nn.2898

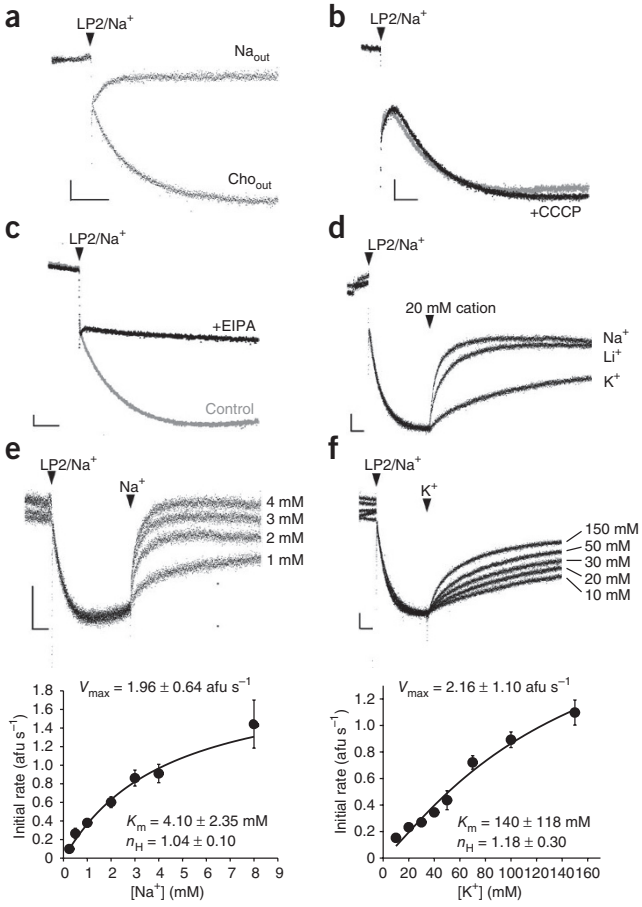

Figure 1 Synaptic vesicles express a Na^+/H^+ exchange activity. (**a**,**b**) Measurement of ΔpH across synaptic vesicles using acridine orange fluorescence. The quenching of fluorescence reflects the generation of an inside-acidic ΔpH. Synaptic vesicles preloaded with Na^+ (LP2/Na^+) and pretreated with bafilomycin to inhibit the V-ATPase were added (time point indicated by arrowhead) to either 150 mM sodium gluconate (Na_{out}) or 150 mM choline gluconate (cho_{out}) (**a**), or to 150 mM choline gluconate buffer with (black) or without (gray) CCCP (**b**). CCCP did not affect the rate or extent of acidification, indicating that the outwardly directed Na^+ gradient does not drive H^+ flux through changes in membrane potential. (**c**) The acidification of synaptic vesicles by an outwardly directed Na^+ gradient was inhibited by EIPA (15 μM). (**d**) The monovalent cations Na^+, Li^+ and K^+ (20 mM) were added to synaptic vesicles that were acidified by an outwardly directed Na^+ gradient. Data are presented as in **a**. (**e**,**f**) After acidification by an outwardly directed Na^+ gradient, synaptic vesicles alkalinized in a dose-dependent manner to Na^+ (**e**) and K^+ (**f**). The mean initial rates of alkalinization varied as a function of cation concentration (bottom, $n = 3$), with V_{max}, K_m and the Hill coefficient (n_H) obtained by fitting to the Hill equation. All horizontal scale bars indicate 30 s and all vertical scale bars indicate 10 afu. Error bars represent s.e.m.

permeation through a channel or by stoichiometrically coupled H^+ exchange[20]. Coupled cation/H^+ exchange has the advantage that it uses ΔpH to drive cation uptake and, if electroneutral, does not dissipate Δψ, allowing the V-ATPase to increase Δψ at the expense of the ΔpH that accumulates during vesicular glutamate transport.

A cation/H^+ exchange mechanism predicts that a cation gradient will drive the formation of ΔpH in the absence of the V-ATPase. To test this hypothesis, we pre-loaded synaptic vesicles (lysate pellet, LP2; see Online Methods) with high Na^+ at pH 7.4, inhibited the H^+ pump with bafilomycin A1 and diluted the vesicles (LP2/Na^+) into buffer (pH 7.4) without Na^+ (**Fig. 1**). Using the quenching of acridine orange fluorescence in acidic compartments, we found that the outwardly directed Na^+ gradient sufficed to acidify synaptic vesicles in the absence of V-ATPase activity, whereas dilution into buffer with Na^+ eliminated this effect, demonstrating its dependence on a Na^+ gradient (**Fig. 1a**).

Although consistent with coupled cation/H^+ exchange, cation-driven acidificaton might simply reflect the development of negative Δψ resulting from the efflux of Na^+, followed by H^+ influx driven by membrane potential. If driven by Δψ, H^+ flux should increase in the presence of the H^+ ionophore carbonyl cyanide chlorophenylhydrazone (CCCP). However, the ratio of the rate of CCCP acidification to the rate of acidification in controls was 0.931 ± 0.069 ($P = 0.42$ by two-tailed, paired t test, $n = 3$; **Fig. 1b**). CCCP had no effect on the rate of acidification, effectively excluding a role for Δψ in the H^+ entry driven by cation efflux. Thus, Na^+ efflux and H^+ influx do not appear to occur through distinct mechanisms, but rather through stoichiometrically coupled and presumably electroneutral exchange.

After the formation of stable ΔpH, addition of external Na^+ alkalinizes the vesicles, demonstrating flux reversal. We took advantage of this phenomenon to compare monovalent cations. At all of the concentrations that we tested (5, 20 and 150 mM), alkalinization was greater for Na^+ and Li^+ than for K^+ (**Fig. 1d** and data not shown). Characterization of the initial rate yielded a K_m of 4.10 ± 2.35 mM for Na^+ and 140 ± 118 mM for K^+ (Hill coefficient = 1.04 ± 0.10 and 1.18 ± 0.30, respectively). The differences in recognition of the two cations presumably account for the inability of K^+ to completely reverse the ΔpH created by an outwardly directed Na^+ gradient, but the V_{max} for both cations was markedly similar (1.96 ± 0.64 arbitrary fluorescent units (afu) s^{-1} for Na^+ versus 2.16 ± 1.10 afu s^{-1} for K^+; **Fig. 1e**,**f**).

To further examine the possibility that cation flux through a channel drives H^+ translocation, we determined whether synaptic vesicles express an endogenous cation conductance. We created an artificial ΔpH by loading the vesicles with ammonium tartrate (100 mM), inhibiting the V-ATPase with bafilomycin and diluting the membranes into buffer lacking NH_4^+; the efflux of NH_3 as a result of dilution rapidly produced ΔpH (**Fig. 2**). The H^+ ionophore CCCP did not dissipate the ΔpH formed by dilution, presumably because after the establishment of ΔpH, the efflux of H^+ rapidly creates lumen-negative Δψ that opposes further efflux (**Fig. 2a**). Furthermore, the inability of CCCP to dissipate ΔpH even after dilution into 150 mM potassium gluconate (**Fig. 2b**) indicates that synaptic vesicles lack an endogenous K^+ channel, which can shunt the developing Δψ. The addition of the K^+ ionophore valinomycin to dilution buffer containing 150 mM K^+ immediately triggered H^+ efflux, which increased in the presence of CCCP, but valinomycin had no effect in buffer lacking K^+ (**Fig. 2**). The inability of K^+ to dissipate ΔpH in the absence of valinomycin excludes a role for endogenous channels in the observed cation-driven H^+ flux by synaptic vesicles.

Cation/H^+ exchange increases synaptic vesicle Δψ

To examine the role of cation/H^+ exchange in the presence of the H^+ pump and specifically on the glutamatergic population of synaptic vesicles, we used ATP and glutamate to acidify synaptic vesicles. In the presence of 1 mM MgATP and 2 mM Cl^- (to activate allosterically the VGLUTs), 10 mM glutamate produced substantial acidification (**Fig. 3a**). This acidification was specific for glutamatergic vesicles, as, under the same conditions, the closely related aspartate (which is not recognized by VGLUTs) causes no acidification[24]. The subsequent addition of 50 mM Na^+ or K^+ produced a steady alkalinization, whereas addition of $NMDG^+$ as a control had no effect (**Fig. 3a**). Similar to the results we obtained in the absence of V-ATPase activity, both cations alkalinized and Na^+ had a greater effect than K^+ at low concentrations (**Fig. 3a**). Acidification by the ATPase increased

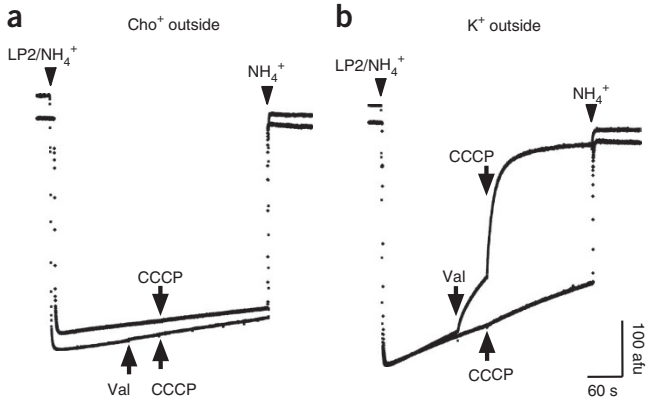

Figure 2 Synaptic vesicles lack a detectable K^+ channel conductance. (**a**,**b**) Measurement of ΔpH across synaptic vesicles using acridine orange fluorescence. Synaptic vesicles were acidified by preloading with 200 mM NH_4^+ (LP2/NH_4^+) and dilution into NH_4^+-free buffer containing no K^+ (cho$^+$ outside, **a**) or 150 mM K^+ (K^+ outside, **b**). In each panel, arrows in the same direction indicate addition to one trace, and arrows in the opposite direction indicate addition to the other trace. CCCP (5 μM) had no effect in the absence of K^+, with or without the addition of 50 nM valinomycin (val). CCCP alone also had no effect in the presence of K^+, indicating the absence of a substantial K^+ conductance. However, the prior addition of valinomycin enabled CCCP to alkalinize the vesicles rapidly, indicating that CCCP would have produced alkalinization in the presence of an endogenous K^+ conductance. Addition of 100 mM NH_4^+ to the external medium immediately reversed the acidification.

the concentration of both cations required for alkalinization, but we found that cation/H^+ exchange could reduce the ΔpH of glutamatergic synaptic vesicles despite the presence of an active H^+ pump.

By selectively dissipating ΔpH, cation/H^+ exchange should increase Δψ generated by the V-ATPase. To measure Δψ, we used the potential-sensitive, ratiometric fluorescent dye oxonol VI, focusing on K^+ because of its physiological relevance as the most abundant cytoplasmic cation. Activation of the V-ATPase with ATP increased the fluorescence ratio of oxonol VI, indicating that a positive membrane potential was formed, and the addition of K^+ (50 mM) caused a further increase of ~40% (**Fig. 3b**). To determine whether Δψ increases as a result of dissipation of ΔpH and secondary activation of the V-ATPase, we used ammonia, which acts as a weak, permeant base to dissipate ΔpH. Ammonium increased the fluorescence ratio of oxonol VI, promoting Δψ as anticipated (**Fig. 3b**). Furthermore, the presence of ammonia reduced the effect of K^+ and vice versa, indicating that they act through a common mechanism. K^+/H^+ exchange across synaptic vesicle membranes thus dissipates ΔpH to increase Δψ.

Monovalent cations increase vesicular glutamate uptake

The ability of cation/H^+ exchange to increase Δψ suggests that cations should stimulate glutamate transport into synaptic vesicles. We compared the effects of potassium gluconate and choline gluconate on ^{3}H-glutamate uptake by synaptic vesicles, using either 2 mM KCl or choline chloride to provide allosteric activation of the VGLUTs. The use of K^+ rather than Na^+ minimized the activity of any contaminating plasma membrane excitatory amino acid transporters, which rely on Na^+ co-transport. Because of the variation in absolute uptake measured on different occasions using different synaptic vesicle preparations (s.d./mean of up to 50%), we normalized the uptake in each experiment to that observed in choline and then averaged the normalized values from independent experiments. External K^+ stimulated glutamate uptake into synaptic vesicles by ~50%, and uptake and stimulation by K^+ were blocked by Evans Blue, an inhibitor of the VGLUTs[26] (**Fig. 4a**). We also observed no specific uptake of ^{3}H-aspartate, which is recognized by the plasma membrane glutamate transporters, but not by the VGLUTs, confirming the specificity of the assay for vesicular glutamate transport. To determine whether the loading of synaptic vesicles with membrane-impermeant choline gluconate has unanticipated consequences, we also examined glutamate uptake after pre-loading with sodium gluconate or the more physiological NaCl, and observed little effect on glutamate uptake, although internal NaCl slightly reduced the stimulatory effect of external K^+ (**Supplementary Fig. 1**). We therefore used vesicles pre-loaded with choline gluconate for all subsequent experiments.

To characterize the effect of K^+ on glutamate uptake, we examined the time course and found that the stimulation by K^+ increased over time, having less effect at 1–2 min than at later time points, when it approached

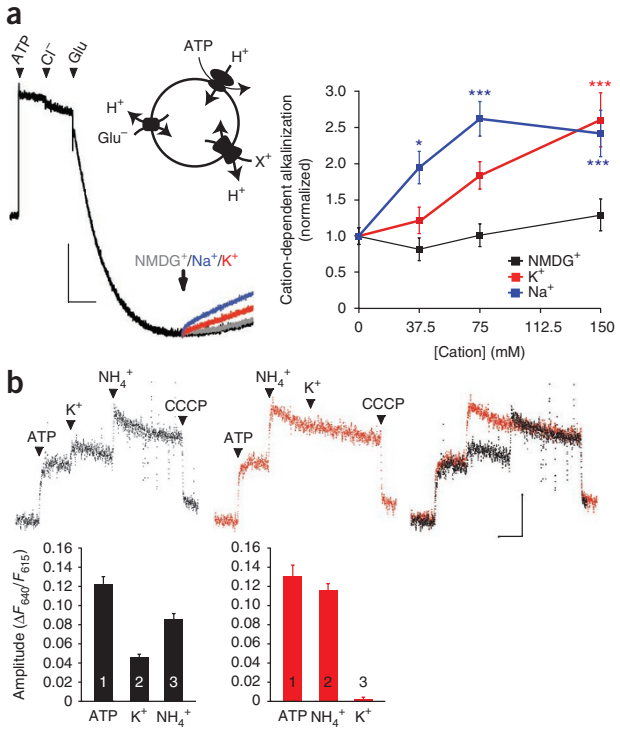

Figure 3 Cation/H^+ exchange activity is present on glutamatergic synaptic vesicles and increases Δψ. (**a**) The quenching of acridine orange fluorescence revealed progressive acidification of 100 μg LP2 protein by 1 mM MgATP, 2 mM choline chloride and 10 mM choline glutamate (left). Gluconate salts of NMDG$^+$ (gray), Na^+ (blue) or K^+ (red) (75 mM final concentration) were added at the arrow and compared with vesicles that received no additional cation (black). The vertical scale bar indicates 30 afu and the horizontal scale bar represents 60 s. The mean fluorescence change 150 s after the arrow shows that Na^+ and K^+, but not NMDG$^+$, reversed acidification in a dose-dependent manner (right). $^*P < 0.05$, $^{***}P < 0.001$ by two-way ANOVA with *post hoc* Bonferroni test (n = 6–12 samples). Glu, glutamate. (**b**) Synaptic vesicle membrane potential was measured using the ratiometric fluorescence of oxonol VI, with an increase in the ratio reflecting greater inside-positive potential. Arrowheads indicate sequential addition of 1 mM MgATP, 50 mM potassium gluconate, 10 mM $(NH_4)_2$ tartrate and 5 μM CCCP (left), with the order of K^+ and NH_4^+ addition reversed in the middle panel, and the two traces superimposed on the right. Bar graphs show the mean change in fluorescence ratio, with the order of addition indicated by numbers on or above the bars (n = 9 and 4 for left and middle panels, respectively; $P < 0.05$ for the effect of NH_4^+ after versus before K^+, and $P < 0.0001$ for the effect of K^+ amplitude before and after NH_4^+, by two-tailed unpaired t test). The vertical scale bar indicates a ratio of 0.10 and the horizontal scale bar represents 60 s. Data are presented as mean ± s.e.m.

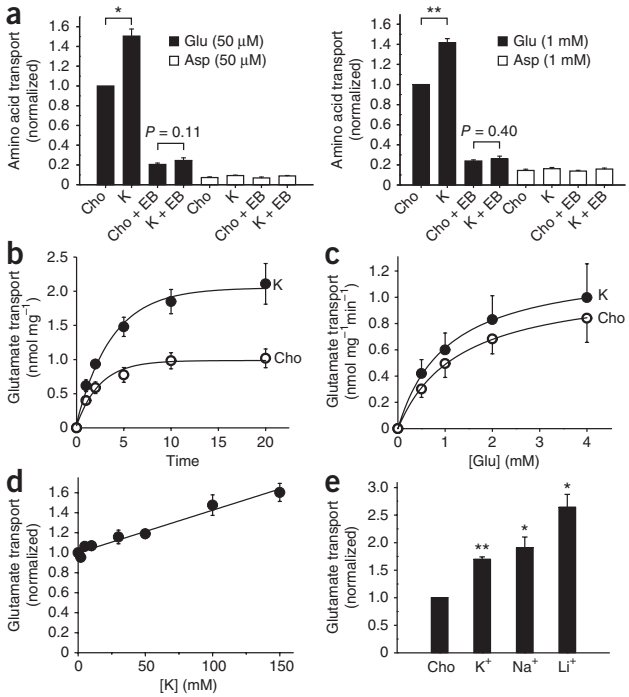

Figure 4 Monovalent cations increase glutamate transport into synaptic vesicles. (**a**) The uptake of ^{3}H-glutamate (filled bars) or ^{3}H-aspartate (open bars) by rat brain synaptic vesicles was measured at 10 min in assay buffer containing either 2 mM choline chloride and 148 mM choline gluconate (cho) or 2 mM KCl and 148 mM potassium gluconate (K), in either 50 μM or 1 mM amino acid, with or without the VGLUT inhibitor Evans Blue (EB) (at 10 and 100 μM for left and right panels, respectively). Uptake was normalized to that observed with choline in the absence of Evans Blue. $^*P < 0.05$, $^{**}P < 0.01$ ($n = 3$). (**b**,**c**) Time course (**b**) and kinetics (**c**) of glutamate uptake in either 150 mM choline (open circles) or 150 mM K^+ (filled circles). The time course was performed using 1 mM glutamate and the kinetic analysis was carried out at 1 min, yielding a mean K_m of 1.02 ± 0.08 mM for K^+ and 1.27 ± 0.04 mM for cho ($P < 0.05$), and a mean V_{max} of 1.26 ± 0.33 nmol mg^{-1} and 1.12 ± 0.24 nmol mg^{-1} for K^+ and cho, respectively ($P = 0.31$) ($n = 3$). (**d**) Dose response of glutamate uptake to potassium, with total choline and potassium gluconate adjusted to 150 mM, and uptake normalized to that observed in the absence of potassium. (**e**) Uptake of 1 mM ^{3}H-glutamate for 10 min in the presence of 150 mM potassium, sodium or lithium gluconate, normalized to that in 150 mM choline ($n = 3$). Statistical analysis was by two-tailed, paired *t* test, and values indicate mean ± s.e.m.

100% after background subtraction (**Fig. 4b**). Consistent with a primary effect on thermodynamic equilibrium, kinetic analysis revealed only a small effect of K^+ on the K_m and no effect on V_{max} (**Fig. 4c**). The analysis of dose response also showed a linear relationship up to 150 mM K^+ (**Fig. 4d**). To assess the effects of Na^+ and Li^+ in this assay, we inhibited any contaminating Na^+-dependent plasma membrane glutamate transporters with DL-*threo*-β-benzyloxyaspartic acid (TBOA; **Supplementary Fig. 2**). Consistent with the results of our acridine orange experiments, we found that Na^+ and Li^+ also stimulated vesicular glutamate uptake (**Fig. 4e**), and the similar effect of all three cations in this assay presumably reflects the use of higher, saturating concentrations (150 mM) at a later time point than were used in the real-time fluorescence measurements of ΔpH (50 mM), where Na^+ and Li^+ had a bigger effect than K^+.

The stimulation of glutamate uptake into synaptic vesicles by monovalent cations could be a result of an allosteric effect on VGLUT activity or an increase in the driving force for transport. Direct allosteric regulation should influence the kinetics of transport or exhibit saturation, but K^+ had little effect on the observed kinetics (**Fig. 4c**), and the dose response to K^+ showed no evidence of saturation (**Fig. 4d**). To determine whether K^+ stimulates glutamate uptake by influencing $\Delta\mu_{H+}$, we again used ammonia to convert ΔpH to Δψ. By itself, 20 mM NH_4^+ stimulated glutamate uptake, consistent with the primary dependence of the VGLUTs on Δψ rather than ΔpH (**Fig. 5a**). The extent of stimulation resembled that produced by 150 mM K^+. We then tested whether K^+ can stimulate glutamate transport in the presence of ammonia and found that, although not eliminated, the stimulation by K^+ was substantially reduced by ammonia (**Fig. 5a**). Conversely, the stimulation by ammonia was reduced by K^+, corroborating our results with oxonol VI, which suggest that potassium and ammonia act through a common mechanism. Given that ammonia dissipates ΔpH, these results suggest that ΔpH is required for the full stimulation by K^+ and that H^+ efflux drives K^+ entry through K^+/H^+ exchange. The residual stimulation of glutamate uptake by K^+ in the presence of NH_4^+ (**Fig. 5a**) can be attributed to the same exchange mechanism that is driven solely by a K^+ gradient rather than by both ΔpH and a K^+ gradient.

To determine whether a cation channel even has the potential to influence vesicular glutamate transport, we measured glutamate uptake in the presence of the K^+ ionophore valinomycin and 15 mM K^+, a concentration of K^+ that had little effect by itself (**Fig. 4d**). Valinomycin had no effect on vesicular glutamate transport under these conditions (**Fig. 5b**) as well as at physiological concentrations of K^+ (data not shown), indicating that, even if a cation channel were present, it would not promote vesicle filling with glutamate. In contrast, the K^+/H^+-exchanging ionophore nigericin markedly increased glutamate uptake even in 15 mM K^+ (**Fig. 5b**), confirming that K^+/H^+ exchange potently stimulates vesicular glutamate transport.

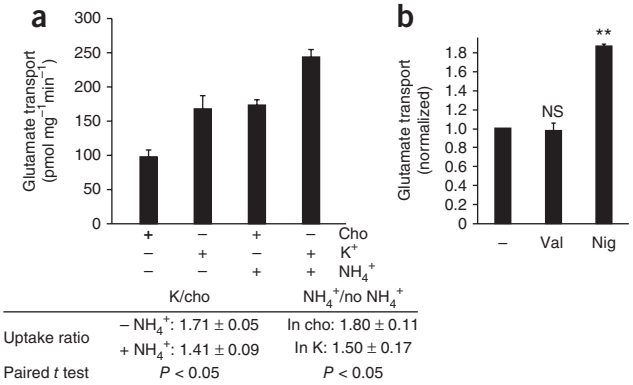

Uptake ratio	– NH_4^+: 1.71 ± 0.05 + NH_4^+: 1.41 ± 0.09	In cho: 1.80 ± 0.11 In K: 1.50 ± 0.17
Paired *t* test	$P < 0.05$	$P < 0.05$

Figure 5 Cation/H^+ exchange stimulates glutamate uptake by increasing Δψ. (**a**) Synaptic vesicle uptake of 1 mM ^{3}H-glutamate was measured in either 150 mM choline or 150 mM K^+, in the presence or absence of 10 mM $(NH_4)_2$tartrate (top). The fold-stimulation of transport by K^+ in the presence or absence of NH_4^+ and by NH_4^+ in the presence or absence of K^+ indicates that NH_4^+ partially occluded the effect of K^+ and vice versa ($P < 0.05$ by two-tailed paired *t* tests, $n = 4$). (**b**) The uptake of ^{3}H-glutamate (1 mM) by synaptic vesicles was measured in 15 mM potassium gluconate/135 mM choline gluconate with or without either 50 nM nigericin (Nig) or 50 nM valinomycin. $^{**}P < 0.01$, NS indicates not significant ($P = 0.76$), two-tailed paired *t* tests ($n = 3$). Values indicate mean ± s.e.m.

Presynaptic K^+ increases quantal size at the calyx of Held

If cations increase glutamate uptake by synaptic vesicles, presynaptic K^+ should influence quantal size. We performed paired recordings at the calyx of Held, a giant glutamatergic terminal in the brainstem auditory pathway in which it is possible to dialyze cytosolic contents by whole-cell patch clamp, and simultaneously measured the postsynaptic response. Given that glutamate receptors at this synapse are not saturated by a single quantum of transmitter[2,3], it should be possible to detect changes in mEPSC amplitude as a result of changes in vesicle filling.

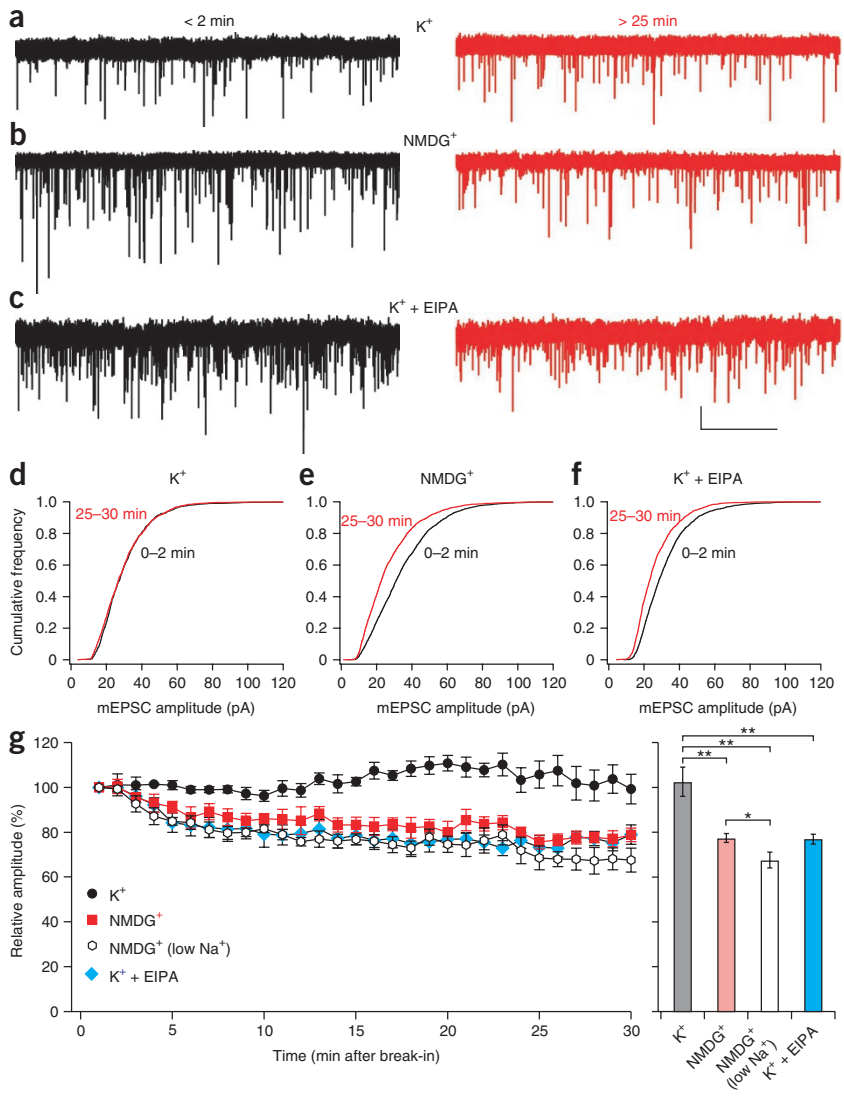

Figure 6 Presynaptic K^+ regulates mEPSC amplitude at the calyx of Held. (**a**–**f**) Paired recordings were performed from both pre- and postsynaptic elements at the calyx of Held. mEPSCs were recorded postsynaptically immediately (within 2 min) and 25–30 min after break-in to the presynaptic terminal with a pipette containing either 130 mM K^+ solution (**a**,**d**), 130 mM $NMDG^+$ (zero K^+) solution (**b**,**e**) or high K^+ solution with 50–100 μM EIPA (**c**,**f**). All presynaptic solutions contained 10 mM Na^+ to mimic physiological conditions. Recordings made <2 min (left) and 25–30 min (right) after break-in to the presynaptic terminal are shown in **a**–**c**. Vertical and horizontal scale bars indicate 20 pA and 2 s, respectively. Cumulative probability histograms of mEPSC amplitude early (black) and late (red) during dialysis of the nerve terminal showed relatively little difference when the pipettes were filled with high K^+ solution ($P > 0.05$, $n = 4$, **d**), but shifted toward smaller amplitudes with a presynaptic solution low in K^+ ($P < 0.001$, $n = 5$, **e**) or with solution containing high K^+ and EIPA ($P < 0.05$, $n = 4$, **f**). (**g**) Time course of the average data from paired recordings with presynaptic pipettes containing high K^+ (black, $n = 4$), low K^+ (red, $n = 5$) or high K^+ solution with 50–100 μM EIPA (blue, $n = 4$). Each point represents the mean and s.e.m. of recording over the previous minute. All presynaptic solutions contained 10 mM Na^+ except for the low Na^+ solution (open, $n = 5$), which contained only 0.6 mM Na^+. $^*P < 0.05$, $^{**}P < 0.01$. Error bars represent s.e.m.

Immediately after break-in to whole-cell mode, we observed no difference in mean mEPSC amplitude with the presynaptic pipette containing either high K^+ or $NMDG^+$ solution ($P = 0.76$). Moreover, with high K^+ solution, the mEPSC remained stable over 25–30 min of recording ($P > 0.05$, $n = 4$; **Fig. 6**). With dialysis of the terminal in $NMDG^+$ rather than K^+, however, mEPSC amplitude gradually declined by over 30% ($P < 0.001$, $n = 5$; **Fig. 6b**,**e**,**g**). Normalized to the values observed immediately after break-in, mEPSC size was clearly lower in $NMDG^+$ than in K^+ ($P < 0.05$), and the cumulative frequency distribution shifted to the left with dialysis in $NMDG^+$, but not K^+ (**Fig. 6d**,**e**). The difference in mEPSC amplitude was notably consistent with the stimulation of vesicular glutamate transport by cations observed *in vitro* using either choline or $NMDG^+$ as a control (**Fig. 4a** and **Supplementary Fig. 3**). As predicted from the dissipation of ΔpH by cations in the presence of an active H^+ pump (**Fig. 3a**) and from the direct measurement of glutamate uptake (**Supplementary Fig. 3**), the presence of 10 mM Na^+ in NMDG did not reproduce the effect of 130 mM K^+ (**Fig. 6**), further supporting the importance of K^+ under physiological conditions.

EIPA inhibits synaptic vesicle cation/H^+ exchange

Stoichiometric cation/H^+ exchange predicts that, just as a cation gradient can drive H^+ flux, a H^+ gradient should also drive the accumulation of cations. We measured the uptake of $^{22}Na^+$ by synaptic vesicles acidified with glutamate to isolate the glutamatergic population. We observe more $^{22}Na^+$ uptake in the presence of glutamate than in the presence of aspartate as a control (**Fig. 7a**), suggesting that vesicle acidification mediated by the VGLUTs drives $^{22}Na^+$ influx. Indeed, the VGLUT inhibitor Evans Blue blocked the stimulation by glutamate (**Fig. 7b**). Although the effect of glutamate appeared to be modest, the ionophore monensin, which directly exchanges H^+ for Na^+, only increased uptake by ~70%, indicating that the endogenous activity is substantial. The V-ATPase inhibitor bafilomycin also blocked glutamate-stimulated $^{22}Na^+$ uptake (**Fig. 7b**), confirming that the uptake depends on $\Delta\mu_{H+}$ generated by the V-ATPase and arguing against a role for a channel, as cation uptake by a channel should increase (rather than decrease) in the absence of a positive $\Delta\psi$ produced by the V-ATPase. Furthermore, the dissipation of ΔpH by ammonia, which should have little effect on a cation channel, blocked the stimulation of $^{22}Na^+$ uptake by glutamate (**Fig. 7b**), consistent with its dependence on ΔpH.

To characterize the proteins responsible for synaptic vesicle cation/H^+ exchange, we took advantage of the available pharmacology. In particular, we compared the effects of glutamate and aspartate on $^{22}Na^+$ uptake in the presence of different inhibitors. The K^+ channel inhibitor tetraethylammonium and Na^+ channel inhibitor tetrodotoxin (TTX), as well as the TRP channel inhibitors ruthenium red and 2-aminoethoxydiphenyl borate (2-APB), had no effect on glutamate-induced $^{22}Na^+$ uptake (**Fig. 7c**), consistent with the idea that a cation channel is not involved.

Coupled cation/H^+ exchange suggests that Na^+/H^+ exchangers (NHEs) are involved. The NHEs include both plasma membrane isoforms involved in the regulation of cell pH and osmolyte

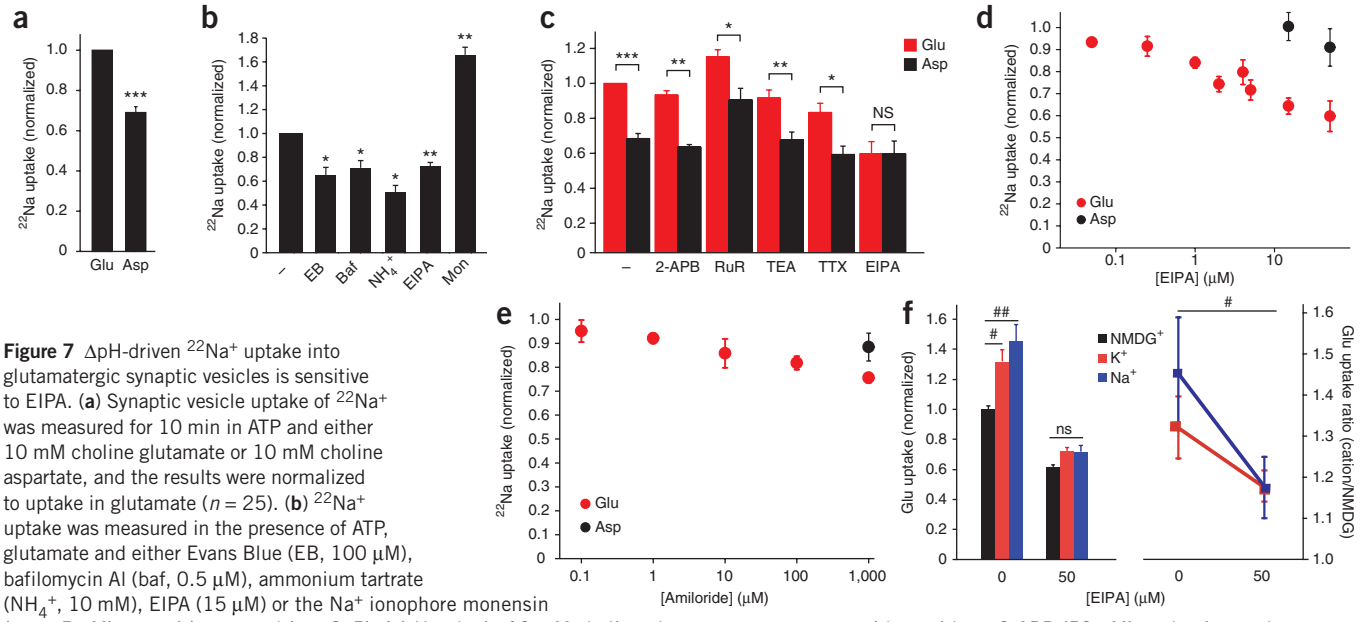

Figure 7 ΔpH-driven $^{22}Na^+$ uptake into glutamatergic synaptic vesicles is sensitive to EIPA. (**a**) Synaptic vesicle uptake of $^{22}Na^+$ was measured for 10 min in ATP and either 10 mM choline glutamate or 10 mM choline aspartate, and the results were normalized to uptake in glutamate ($n = 25$). (**b**) $^{22}Na^+$ uptake was measured in the presence of ATP, glutamate and either Evans Blue (EB, 100 μM), bafilomycin A1 (baf, 0.5 μM), ammonium tartrate (NH_4^+, 10 mM), EIPA (15 μM) or the Na^+ ionophore monensin (mon, 5 μM) as positive control ($n = 3$–5). (**c**) Uptake in 10 mM choline glutamate or aspartate, with or without 2-APB (50 μM), ruthenium red (RuR, 100 μM), tetraethylammonium (TEA, 5 mM), TTX (0.5 μM) and EIPA (50 μM) ($n = 3$–5). (**d**) EIPA inhibited $^{22}Na^+$ uptake more potently in vesicles acidified with glutamate ($n = 3$–6). (**e**) Amiloride also inhibited $^{22}Na^+$ uptake, but less potently than EIPA ($n = 5$–6). $^*P < 0.05$, $^{**}P < 0.01$ and $^{***}P < 0.0001$; NS indicates $P = 0.99$ by two-tailed paired t tests. (**f**) The uptake of ^{3}H-glutamate was measured for 10 min in assay buffer containing 4 mM MgATP, 2 mM choline chloride, 10 mM glutamate, 10 mM NMDG gluconate, and either 150 mM NMDG gluconate (black), 150 mM sodium gluconate (blue) or 150 mM potassium gluconate (red), with or without EIPA. After subtraction of the background in 100 μM Evans Blue, uptake was normalized to that observed in NMDG gluconate without EIPA (left). The uptake in Na^+ or K^+ was then normalized to that in $NMDG^+$ (right). $^{\#}P < 0.05$, $^{\#\#}P < 0.01$ by two-way ANOVA ($n = 15$–18); ns, $P > 0.33$. Data indicate mean ± s.e.m.

concentration and intracellular isoforms that recognize K^+ as well as Na^+, but remain poorly understood in terms of their physiological role[27,28]. In general, the NHEs are sensitive to inhibition by the amiloride analog 5-(N-ethyl-N-isopropyl)amiloride (EIPA)[28]. However, most studies of NHE pharmacology have examined the uptake of trace $^{22}Na^+$, requiring only low micromolar or submicromolar concentrations of compounds such as EIPA that act as competitive inhibitors. Physiological levels of Na^+ or K^+ would require much higher concentrations of EIPA, at which nonspecific effects may arise. Thus, we used $^{22}Na^+$ to assess the EIPA sensitivity of cation uptake by synaptic vesicles. EIPA inhibited glutamate-activated $^{22}Na^+$ uptake in the very low micromolar range and had no effect at much higher concentrations in the presence of aspartate (**Fig. 7d**), indicating that uptake inhibition by EIPA occurs specifically at glutamatergic vesicles. EIPA also inhibited $^{22}Na^+$ uptake more potently than amiloride (**Fig. 7e**), a feature that is characteristic of the NHEs[28]. In addition, we tested the effect of EIPA on cation stimulation of vesicular glutamate uptake. Using higher concentrations of EIPA (50 μM) to compete with the higher concentrations of cation that we used (150 mM), we found that EIPA also inhibited the stimulation of glutamate uptake by Na^+ and K^+ (**Fig. 7f**). Furthermore, EIPA inhibited the cation/H^+ exchange activity that was responsible for the Na^+ gradient–driven flux of H^+ that we observed in the acridine orange assay (**Fig. 1c**). NHEs therefore appear to mediate the stimulation of vesicular glutamate transport by cation/H^+ exchange.

To assess the dependence of quantal size on NHE activity, we used the calyx of Held. Given that the presynaptic solution contained 130 mM K^+ rather than the trace amounts of $^{22}Na^+$ that we used to measure flux, we added 50–100 μM EIPA to the presynaptic pipette. Dialysis with a high K^+ solution containing EIPA gradually reduced mEPSC amplitude compared with dialysis of the same solution without EIPA ($P < 0.01$, $n = 4$; **Fig. 6c,f,g**), similar to what was seen in the low K^+ solution. Thus, EIPA inhibits the effect of K^+ on quantal size, supporting the involvement of an intracellular NHE.

DISCUSSION

Our results reveal a previously unknown presynaptic mechanism for the regulation of quantal size (**Supplementary Fig. 4**). During vesicular glutamate transport, ΔpH accumulates, opposing the activity of the H^+ pump and therefore limiting the storage of glutamate. Cation/H^+ exchange dissipates ΔpH, but, as a result of its electroneutrality, spares Δψ. As a result, continuing activity of the V-ATPase selectively increases Δψ, effectively converting ΔpH into Δψ. Given that vesicular glutamate transport depends primarily on Δψ, electroneutral cation/H^+ exchange increases vesicle filling with glutamate.

Several of our observations suggest that there is electroneutral cation/H^+ exchange activity in synaptic vesicles. First, the efflux of preloaded cation down a concentration gradient drove H^+ entry, suggesting that cation flux is directly coupled to H^+ exchange. Alternatively, this might reflect the production of negative Δψ by cation efflux, followed by the Δψ-driven H^+ influx, but the H^+ ionophore CCCP affected neither the rate nor the extent of acidification, effectively excluding a Δψ-driven process. A high-conductance H^+ channel might occlude the effect of CCCP, and synaptic vesicles can exhibit a H^+ leak. However, CCCP greatly increased H^+ efflux in the presence of an electrical shunt (**Fig. 2**), indicating that the endogenous H^+ conductance cannot occlude the effect of the ionophore. CCCP should have stimulated H^+ entry if it depended on Δψ, and the lack of an effect supports the idea that there is direct, electroneutral cation/H^+ coupling.

Second, we did not detect a cation conductance on synaptic vesicles. CCCP did not dissipate ΔpH produced by the efflux of NH_3 because the development of negative Δψ opposes net H^+ efflux. This was true even in the presence of external K^+, indicating that cation entry through endogenous channels cannot shunt the developing Δψ.

Only the addition of K^+ ionophore valinomycin in the presence of external K^+ allowed substantial H^+ efflux, indicating that we would have detected an endogenous cation channel if one were present. Although we cannot exclude the presence of a cation channel on synaptic vesicles, our results suggest that any conductance must be small.

Third, inhibition of the V-ATPase with bafilomycin reduced $^{22}Na^+$ uptake. Given that V-ATPase activity makes $\Delta\psi$ more positive, cation uptake through a channel should increase if the V-ATPase is inhibited. The reduction that we observed in $^{22}Na^+$ uptake by bafilomycin suggests that $\Delta\psi$ does not drive flux. Instead, the decrease in $^{22}Na^+$ uptake produced by ammonia supports a selective role for ΔpH, consistent with cation/H^+ exchange. Although electroneutral, cation/H^+ exchange and the resulting dissipation of ΔpH activated the V-ATPase, shifting the expression of $\Delta\mu_{H+}$ from ΔpH to $\Delta\psi$. Indeed, oxonol VI fluorescence revealed the effect of K^+ on $\Delta\psi$, and the occlusion of this effect by ammonia suggests that K^+, similar to NH_4^+, increases $\Delta\psi$ by decreasing ΔpH. Taken together, these results indicate that, in the presence of an active V-ATPase, a stoichiometrically coupled, electroneutral cation/H^+ exchange mechanism increases $\Delta\psi$. By acidifying synaptic vesicles with glutamate, we found that cation/H^+ exchange occurred in the glutamatergic population.

Cation/H^+ exchange provides a mechanism for converting the ΔpH produced by glutamate accumulation back into $\Delta\psi$ that drives vesicular glutamate transport. Indeed, we found that K^+ increased the uptake of glutamate into synaptic vesicles in a manner consistent with thermodynamic effects on the driving force. The time course revealed greater stimulation by K^+ at later time points, and K^+ had no effect on V_{max}, although it did reduce K_m slightly. Although a kinetic parameter, the K_m of vesicular glutamate transport has previously been shown to correlate with $\Delta\psi$[29]. Thus, effect of K^+ on K_m may reflect a change in $\Delta\psi$.

To determine whether the stimulation of VGLUT activity by K^+ involves the observed increase in $\Delta\psi$, we again used ammonia. Similar to K^+, ammonia stimulated glutamate uptake, and the two effects partially occluded each other, suggesting that dissipation of ΔpH accounts for the stimulation by K^+, consistent with cation/H^+ exchange. Alternatively, K^+ influx through a channel could increase $\Delta\psi$ and reduce ΔpH by inhibiting the H^+ pump. Indeed, recent work has suggested that the cation channel TRPM7 found on cholinergic synaptic vesicles is involved in the regulation of acetylcholine release, but this was attributed to protein-protein interactions and changes in release rather than to vesicle filling[30]. We would not have detected the effect of a cation channel expressed on a small subset of synaptic vesicles, but found no evidence for a functional cation channel on the majority of synaptic vesicles. Furthermore, valinomycin did not enable K^+ to stimulate vesicular glutamate transport, indicating that a channel would not increase vesicle filling even if one were present. In contrast, nigericin strongly augmented glutamate uptake, demonstrating the potency of electroneutral K^+/H^+ exchange.

The manipulation of presynaptic cytosol at the calyx of Held further supports a physiological role for vesicle K^+ flux in glutamate release. Dialysis of the presynaptic terminal with a solution containing $NMDG^+$ rather than K^+ reduced quantal size, and the magnitude of the effect resembles that observed biochemically. Although the parallel effects *in vitro* and *in vivo* might not seem surprising, manipulation of presynaptic Cl^- at the calyx of Held does not affect quantal size[31], despite considerable previous work *in vitro* that found a role for Cl^- in the allosteric regulation of VGLUTs[23,29]. Allosteric regulation by Cl^- presumably affects kinetics rather than thermodynamics, and equilibrium may be more important in the determination of quantal size. Cation/H^+ exchange appears to have a greater effect on glutamatergic neurotransmission than the extensively documented effects of Cl^-.

The results suggest that an intracellular NHE is involved in transmitter release. NHEs catalyze the electroneutral exchange of cation for H^+ (1:1), and plasma membrane isoforms (NHE1–5), which recognize Na^+ but not K^+, are important for the regulation of cytoplasmic pH[28]. In contrast, the intracellular isoforms NHE6–9 recognize both K^+ and Na^+ (refs. 32–34), and remain poorly understood. The intracellular yeast homolog Nhx1 contributes to Na^+ resistance and membrane trafficking[35,36]. In mammalian vestibular hair cells, which are surrounded by endolymph containing high concentrations of K^+, a fraction of NHE6 and NHE9 on the plasma membrane regulates cell pH[32]. However, we understand little about the physiological role of NHEs on intracellular membranes.

The apparent electroneutrality of synaptic vesicle cation/H^+ exchange and its recognition of K^+ and Na^+ suggest that there is an active intracellular NHE. The sensitivity of $^{22}Na^+$ uptake by synaptic vesicles to low micromolar concentrations of EIPA, but not to a series of known channel blockers, support the idea that an intracellular NHE is involved[28]. Furthermore, EIPA blocked the ability of high presynaptic K^+ to maintain mEPSC amplitude at the calyx of Held. Together with the characterization of synaptic vesicle cation/H^+ exchange activity, these findings implicate an intracellular NHE in the determination of quantal size. Notably, the endosomal isoforms NHE6 and NHE9 have recently been implicated in brain development and human disease. Mutations in *SLC9A6* (NHE6) cause an X-linked recessive form of mental retardation with seizures[37], and polymorphisms in *SLC9A9* (NHE9) have been associated with autism[38]. Genetic association studies have also implicated NHE9 in attention-deficit/hyperactivity disorder[39]. The role of NHE activity in filling synaptic vesicles with glutamate raises the possibility that these mutations may interfere with behavior by disrupting neurotransmitter release. Although not originally identified in a proteomic analysis of synaptic vesicles[40], NHE6 was recently found in synaptic vesicles storing both GABA and glutamate[41]. Furthermore, recent work in *C. elegans* found that an NHE homolog is involved in chemical signaling from intestinal epithelial cells to muscle[42]. In this case, protons are the signal, and their release does not require vesicle fusion. Instead, cation/H^+ exchange by synaptic vesicles may have evolved from this mechanism.

Our results describe a mechanism for controlling the expression of $\Delta\mu_{H+}$ as either ΔpH or $\Delta\psi$ and suggest a previously unknown intracellular role for NHEs. Although differences in the subcellular location of Cl^- channel (ClC) isoforms might contribute to the variation in pH of different membranes, the lysosomal transporter ClC-7 and a bacterial homolog both exhibit a stoichiometry of 2 Cl^-: 1 H^+ (refs. 43,44), and intracellular isoforms ClC-4 and ClC-5 show similar H^+ coupling[45,46]. It seems unlikely that differences in coupling stoichiometry by the intracellular ClCs can account for the observed variation in organelle pH. However, the combination of a ClC with opposing NHE activity that converts ΔpH back into $\Delta\psi$ could provide an explanation for the wide range of ΔpH: dominance of NHE over ClC activity may confer the relatively small ΔpH of early endosomes, and dominance of ClC over NHE could confer the larger ΔpH of late endosomes and lysosomes. Consistent with this hypothesis, none of the intracellular NHEs have yet been localized to lysosomes; NHE6 and 9 reside earlier in the endocytic pathway and NHE7 and 8 are present in the Golgi complex[33,34]. Thus, the regulation of NHE and ClC trafficking may contribute to the observed variation in ΔpH across membranes of the secretory pathway.

In addition, intracellular NHE activity has the potential to augment $\Delta\psi$ to a greater extent than predicted by the activity of the H^+-ATPase alone. Electroneutral K^+/H^+ exchange predicts $\log_{10}([H^+]_i/[H^+]_o) = \log_{10}([K^+]_i/[K^+]_o)$ at equilibrium, and assuming the H^+ pump can create $\Delta\mu_{H+} = (\log_{10}([H^+]_i/[H^+]_o) + \Delta\psi/(2.3RT/F)) \sim 3$, where R is the gas constant, T is the absolute temperature and F is Faraday's constant, $3 - \log_{10}([H^+]_i/[H^+]_o) = \Delta\psi/(2.3RT/F)$ or $3 + \log_{10}([K^+]_o/[K^+]_i) = \Delta\psi/(2.3RT/F)$.

A tenfold inwardly directed gradient of K^+ would thus increase the maximum $\Delta\psi$ possible by ~60 mV. Rather than simply modulating the expression of $\Delta\mu_{H+}$ as either ΔpH or $\Delta\psi$, intracellular NHE activity, together with an inwardly directed K^+ gradient, can augment the membrane potential produced by the vacuolar H^+ pump.

The focus of most previous work on ΔpH rather than $\Delta\psi$ reflects the established role of ΔpH in processes such as ligand-receptor dissociation and lysosomal degradation. However, the importance of $\Delta\psi$ for vesicular glutamate transport and the identification of cation/H^+ exchange as a mechanism for promoting $\Delta\psi$ suggest that changes in $\Delta\psi$ may not simply reflect the unintended consequence of regulating ΔpH. Instead, $\Delta\psi$ across membranes of the secretory pathway may serve as the primary driving force for additional processes that remain poorly understood.

METHODS

Methods and any associated references are available in the online version of the paper at http://www.nature.com/natureneuroscience/.

Note: Supplementary information is available on the Nature Neuroscience website.

ACKNOWLEDGMENTS

We thank J. Orlowski, S. Schuldiner and members of the Edwards laboratory for many thoughtful discussions, S. Manandhar and F. Farrimond for technical assistance, and R.P. Seal for critical reading of the manuscript. This work was supported by fellowships from A*STAR (to G.Y.G.) and the American Heart Association (to L.B.), and by grants from the National Institute on Deafness and Other Communication Disorders and the National Institute of Neurological Disorders and Stroke (to L.O.T.), and from the National Institute of Mental Health and the National Institute on Drug Abuse (to R.H.E.).

AUTHOR CONTRIBUTIONS

The biochemical experiments were conducted by G.Y.G., J.U. and T.S.H. in the laboratory of R.H.E. L.B. developed the measurement of $^{22}Na^+$ uptake. The electrophysiology experiments were performed by H.H. in the laboratory of L.O.T.

COMPETING FINANCIAL INTERESTS

The authors declare no competing financial interests.

Published online at http://www.nature.com/natureneuroscience/.
Reprints and permissions information is available online at http://www.nature.com/reprints/index.html.

1. Bredt, D.S. & Nicoll, R.A. AMPA receptor trafficking at excitatory synapses. *Neuron* **40**, 361–379 (2003).
2. Ishikawa, T., Sahara, Y. & Takahashi, T. A single packet of transmitter does not saturate postsynaptic glutamate receptors. *Neuron* **34**, 613–621 (2002).
3. Wu, X.S. *et al.* The origin of quantal size variation: vesicular glutamate concentration plays a significant role. *J. Neurosci.* **27**, 3046–3056 (2007).
4. Conti, R. & Lisman, J. The high variance of AMPA receptor– and NMDA receptor–mediated responses at single hippocampal synapses: evidence for multiquantal release. *Proc. Natl. Acad. Sci. USA* **100**, 4885–4890 (2003).
5. Sargent, P.B., Saviane, C., Nielsen, T.A., DiGregorio, D.A. & Silver, R.A. Rapid vesicular release, quantal variability, and spillover contribute to the precision and reliability of transmission at a glomerular synapse. *J. Neurosci.* **25**, 8173–8187 (2005).
6. Karunanithi, S., Marin, L., Wong, K. & Atwood, H.L. Quantal size and variation determined by vesicle size in normal and mutant *Drosophila* glutamatergic synapses. *J. Neurosci.* **22**, 10267–10276 (2002).
7. Steinert, J.R. *et al.* Experience-dependent formation and recruitment of large vesicles from reserve pool. *Neuron* **50**, 723–733 (2006).
8. De Gois, S. *et al.* Homeostatic scaling of vesicular glutamate and GABA transporter expression in rat neocortical circuits. *J. Neurosci.* **25**, 7121–7133 (2005).
9. Wojcik, S.M. *et al.* An essential role for vesicular glutamate transporter 1 (VGLUT1) in postnatal development and control of quantal size. *Proc. Natl. Acad. Sci. USA* **101**, 7158–7163 (2004).
10. Moechars, D. *et al.* Vesicular glutamate transporter VGLUT2 expression levels control quantal size and neuropathic pain. *J. Neurosci.* **26**, 12055–12066 (2006).
11. Seal, R.P. *et al.* Sensorineural deafness and seizures in mice lacking vesicular glutamate transporter 3. *Neuron* **57**, 263–275 (2008).
12. Fremeau, R.T. Jr. *et al.* Vesicular glutamate transporters 1 and 2 target to functionally distinct synaptic release sites. *Science* **304**, 1815–1819 (2004).
13. Daniels, R.W. *et al.* A single vesicular glutamate transporter is sufficient to fill a synaptic vesicle. *Neuron* **49**, 11–16 (2006).
14. Brunk, I. *et al.* The first luminal domain of vesicular monoamine transporters mediates G protein–dependent regulation of transmitter uptake. *J. Biol. Chem.* **281**, 33373–33385 (2006).
15. Saroussi, S. & Nelson, N. Vacuolar H^+-ATPase: an enzyme for all seasons. *Pflugers Arch.* **457**, 581–587 (2009).
16. Johnson, R.G., Carty, S.E. & Scarpa, A. Proton: substrate stoichiometries during active transport of biogenic amines in chromaffin ghosts. *J. Biol. Chem.* **256**, 5773–5780 (1981).
17. Knoth, J., Zallakian, M. & Njus, D. Stoichiometry of H^+-linked dopamine transport in chromaffin granule ghosts. *Biochemistry* **20**, 6625–6629 (1981).
18. Parsons, S.M. Transport mechanisms in acetylcholine and monoamine storage. *FASEB J.* **14**, 2423–2434 (2000).
19. Johnson, R.G., Pfister, D., Carty, S.E. & Scarpa, A. Biological amine transport in chromaffin ghosts. Coupling to the transmembrane proton and potential gradients. *J. Biol. Chem.* **254**, 10963–10972 (1979).
20. Maycox, P.R., Deckwerth, T., Hell, J.W. & Jahn, R. Glutamate uptake by brain synaptic vesicles. Energy dependence of transport and functional reconstitution in proteoliposomes. *J. Biol. Chem.* **263**, 15423–15428 (1988).
21. Tabb, J.S., Kish, P.E., Van Dyke, R. & Ueda, T. Glutamate transport into synaptic vesicles. *J. Biol. Chem.* **267**, 15412–15418 (1992).
22. Van Dyke, R.W. Proton pump-generated electrochemical gradients in rat liver multivesicular bodies. Quantitation and effects of chloride. *J. Biol. Chem.* **263**, 2603–2611 (1988).
23. Hartinger, J. & Jahn, R. An anion binding site that regulates the glutamate transporter of synaptic vesicles. *J. Biol. Chem.* **268**, 23122–23127 (1993).
24. Hnasko, T.S. *et al.* Vesicular glutamate transport promotes dopamine storage and glutamate corelease in vivo. *Neuron* **65**, 643–656 (2010).
25. Schenck, S., Wojcik, S.M., Brose, N. & Takamori, S. A chloride conductance in VGLUT1 underlies maximal glutamate loading into synaptic vesicles. *Nat. Neurosci.* **12**, 156–162 (2009).
26. Chaudhry, F.A., Boulland, J.L., Jenstad, M., Bredahl, M.K. & Edwards, R.H. Pharmacology of neurotransmitter transport into secretory vesicles. *Handb. Exp. Pharmacol.* **184**, 77–106 (2008).
27. Brett, C.L., Donowitz, M. & Rao, R. Evolutionary origins of eukaryotic sodium/proton exchangers. *Am. J. Physiol. Cell Physiol.* **288**, C223–C239 (2005).
28. Orlowski, J. & Grinstein, S. Diversity of the mammalian sodium/proton exchanger SLC9 gene family. *Pflugers Arch.* **447**, 549–565 (2004).
29. Wolosker, H., de Souza, D.O. & de Meis, L. Regulation of glutamate transport into synaptic vesicles by chloride and proton gradient. *J. Biol. Chem.* **271**, 11726–11731 (1996).
30. Krapivinsky, G., Mochida, S., Krapivinsky, L., Cibulsky, S.M. & Clapham, D.E. The TRPM7 ion channel functions in cholinergic synaptic vesicles and affects transmitter release. *Neuron* **52**, 485–496 (2006).
31. Price, G.D. & Trussell, L.O. Estimate of the chloride concentration in a central glutamatergic terminal: a gramicidin perforated-patch study on the calyx of Held. *J. Neurosci.* **26**, 11432–11436 (2006).
32. Hill, J.K. *et al.* Vestibular hair bundles control pH with (Na^+, K^+)/H^+ exchangers NHE6 and NHE9. *J. Neurosci.* **26**, 9944–9955 (2006).
33. Nakamura, N., Tanaka, S., Teko, Y., Mitsui, K. & Kanazawa, H. Four Na^+/H^+ exchanger isoforms are distributed to Golgi and post-Golgi compartments and are involved in organelle pH regulation. *J. Biol. Chem.* **280**, 1561–1572 (2005).
34. Numata, M. & Orlowski, J. Molecular cloning and characterization of a novel (Na^+,K^+)/H^+ exchanger localized to the trans-Golgi network. *J. Biol. Chem.* **276**, 17387–17394 (2001).
35. Ali, R., Brett, C.L., Mukherjee, S. & Rao, R. Inhibition of sodium/proton exchange by a Rab-GTPase–activating protein regulates endosomal traffic in yeast. *J. Biol. Chem.* **279**, 4498–4506 (2004).
36. Brett, C.L., Tukaye, D.N., Mukherjee, S. & Rao, R. The yeast endosomal Na^+K^+/H^+ exchanger Nhx1 regulates cellular pH to control vesicle trafficking. *Mol. Biol. Cell* **16**, 1396–1405 (2005).
37. Gilfillan, G.D. *et al.* SLC9A6 mutations cause X-linked mental retardation, microcephaly, epilepsy and ataxia, a phenotype mimicking Angelman syndrome. *Am. J. Hum. Genet.* **82**, 1003–1010 (2008).
38. Morrow, E.M. *et al.* Identifying autism loci and genes by tracing recent shared ancestry. *Science* **321**, 218–223 (2008).
39. Franke, B., Neale, B.M. & Faraone, S.V. Genome-wide association studies in ADHD. *Hum. Genet.* **126**, 13–50 (2009).
40. Takamori, S. *et al.* Molecular anatomy of a trafficking organelle. *Cell* **127**, 831–846 (2006).
41. Grønborg, M. *et al.* Quantitative comparison of glutamatergic and GABAergic synaptic vesicles unveils selectivity for few proteins including MAL2, a novel synaptic vesicle protein. *J. Neurosci.* **30**, 2–12 (2010).
42. Beg, A.A., Ernstrom, G.G., Nix, P., Davis, M.W. & Jorgensen, E.M. Protons act as a transmitter for muscle contraction in *C. elegans*. *Cell* **132**, 149–160 (2008).
43. Accardi, A. & Miller, C. Secondary active transport mediated by a prokaryotic homologue of ClC Cl- channels. *Nature* **427**, 803–807 (2004).
44. Graves, A.R., Curran, P.K., Smith, C.L. & Mindell, J.A. The Cl^-/H^+ antiporter ClC-7 is the primary chloride permeation pathway in lysosomes. *Nature* **453**, 788–792 (2008).
45. Picollo, A. & Pusch, M. Chloride/proton antiporter activity of mammalian CLC proteins ClC-4 and ClC-5. *Nature* **436**, 420–423 (2005).
46. Scheel, O., Zdebik, A.A., Lourdel, S. & Jentsch, T.J. Voltage-dependent electrogenic chloride/proton exchange by endosomal CLC proteins. *Nature* **436**, 424–427 (2005).

ONLINE METHODS

Materials. Bafilomycin A1 was obtained from EMD Biosciences, oxonol VI from Invitrogen and other chemicals from Sigma. ^{22}NaCl and [^{3}H]L-glutamate were obtained from PerkinElmer and HT-200 Tuffryn filters and Supor 200 filters were from Pall. Choline gluconate was made by titration of choline bicarbonate with gluconic acid to pH 7.4, choline glutamate and choline aspartate by titration of choline base with glutamic or aspartic acid, respectively.

Synaptic vesicle preparation. Synaptic vesicles were isolated by differential centrifugation from rat brain synaptosomes lysed in hypotonic buffer, as described previously[47]. Briefly, the brains of 16 4-week-old Sprague-Dawley rats were homogenized in 320 mM sucrose, 4 mM HEPES-Tris, pH 7.4, 1 mM $MgCl_2$, 1 mM EGTA (homogenization buffer) containing 1 μg ml^{-1} pepstatin A and 200 μM PMSF using nine strokes of a Kontes #22 glass-Teflon homogenizer at 900 r.p.m. After sedimentation at 1,000 g_{max} for 10 min, the supernatant was collected, re-centrifuged at 12,000 g_{max} for 15 min, and the resulting supernatant, as well as the dark brown middle part of the pellet, were discarded. The remaining pellet was washed by resuspension in 6 ml of homogenization buffer per brain, sedimented at 13,000 g_{max} for 15 min, and we again discarded the supernatant and dark brown part of the pellet. The pellet was then resuspended in 0.6 of ml homogenization buffer per brain, and nine volumes of ice-cold water added along with 1 M HEPES-Tris, pH 7.4 to a final concentration of 8 mM. After incubation on ice for 30 min, the suspension was homogenized using five strokes at 3,000 r.p.m. and centrifuged at 33,000 g_{max} for 20 min. The supernatant was immediately collected and centrifuged at 260,000 g_{max} for 2 h. The resultant pellet (lysate pellet, LP2) was resuspended in 400–500 μl of 150 mM choline gluconate containing 10 mM HEPES-Tris, pH 7.4 (or other buffers as specified in **Figs. 1** and **2** and **Supplementary Fig. 1**) by pipetting through progressively narrower micropipette tips, and finally by three passes through a 25 gauge needle. LP2 was frozen in liquid N_2 for storage at −80 °C and thawed on ice before use. Protein concentration was determined using the Bradford assay with bovine serum albumin as the standard. To assess loading with K^+ by freeze-thaw, we titrated with external K^+ in the presence of nigericin to determine the external concentration that eliminated net H^+ flux, as measured by acridine orange fluorescence (see below). Freeze-thaw in 150 mM potassium gluconate resulted in only 25–50 mM lumenal K^+ (data not shown), and we presume that other cations behave similarly. These experiments were approved by the University of California San Francisco Institutional Animal Care and Use Committee.

ΔpH and Δψ measurements. ΔpH and Δψ were measured by acridine orange and oxonol VI fluorescence, respectively. We added 100–200 μg LP2 to 1.5 ml of 150 mM choline or NMDG gluconate (unless otherwise indicated), 10 mM HEPES-Tris, pH 7.4, and either 5 μM acridine orange or 100 nM oxonol VI, and stirred the reaction at 30 °C. A decrease in the fluorescence of acridine orange reflects the generation of an inside-acidic ΔpH; an increase in the fluorescence ratio of oxonol VI reflects the generation of an inside-positive Δψ. In the experiments using LP2 loaded with high Na^+ (which did not involve MgATP), 4 mM $MgSO_4$ and 0.5 μM bafilomycin A1 were included in the external solution. Acridine orange fluorescence was excited at 492 nm and emission was detected at 530 nm; oxonol VI was excited at 560 nm and emission was detected at 640 and 615 nm using a Hitachi F-4500 fluorescence spectrophotometer.

Glutamate transport assay. Unless indicated otherwise, the standard assay buffer for glutamate uptake contained 148 mM choline, NMDG, sodium gluconate or potassium gluconate, 2 mM choline or KCl, 4 mM MgATP, 10 mM HEPES-Tris, pH 7.4, 1 mM choline glutamate (unless otherwise indicated), and 40 μCi ml^{-1} [^{3}H]L-glutamate. When specified, sodium gluconate and lithium gluconate were used at 150 mM and $(NH_4)_2$ tartrate at 10 mM. Transport was initiated by the addition of 100 μg LP2 protein to 200 μl reaction buffer (pre-warmed to 30 °C), and the reaction was incubated at 30 °C for 10 min (unless otherwise indicated) and stopped by rapid filtration and washing four times with 2 ml cold 150 mM HEPES-Tris, pH 7.4. Radioactivity was detected by liquid scintillation, and background transport was measured in the presence of 100 μM Evans Blue subtracted from the data unless otherwise specified. In each experiment, each condition was assayed in triplicate and at least three independent experiments were performed using at least two different synaptic vesicle preparations.

$^{22}Na^+$ transport assay. The standard assay buffer for $^{22}Na^+$ transport contained 148 mM choline gluconate, 2 mM choline chloride, 10 mM choline glutamate, 4 mM MgATP, 10 mM HEPES-Tris, pH 7.4, 0.1 mM ouabain, 0.1 mM bumetanide and 175 nM ^{22}NaCl (5 μCi ml^{-1}). Transport was initiated by adding 100 μg LP2 to 200 μl reaction buffer (pre-warmed to 30 °C). The mixture was incubated at 30 °C for 10 min (unless otherwise indicated) and the reaction stopped by rapid filtration followed by four washes with 1.5 ml cold 150 mM HEPES-Tris, pH 7.4. Radioactivity was detected by liquid scintillation, and nonspecific background at 0 min subtracted from all the data presented. At least three independent experiments were performed, each in triplicate.

mEPSC recordings. The handling and care of animals for these experiments was in accordance with procedures approved by the Institutional Animal Care and Use Committee of Oregon Health Sciences University. We prepared 180–200-μm-thick coronal slices containing the medial nucleus of the trapezoid body from P9–12 Wistar rats as previously described[48,49]. Slices were cut in cold artificial cerebrospinal fluid (ACSF) consisting of 230 mM sucrose, 25 mM glucose, 2.5 mM KCl, 3 mM $MgCl_2$, 0.1 mM $CaCl_2$, 1.25 mM NaH_2PO_4, 25 mM $NaHCO_3$, 0.4 mM ascorbic acid, 3 mM *myo*-inositol and 2 mM sodium pyruvate, pH 7.4, bubbled with 5% CO_2/95% O_2), incubated for 30–60 min at 35 °C and thereafter at 21–23° C.

Slices were transferred to a recording chamber and perfused with recording ACSF containing 125 mM NaCl, 2.5 mM KCl, 2 mM $CaCl_2$, 1 mM $MgCl_2$, 1.25 mM NaH_2PO_4, 0.4 mM ascorbic acid, 3 mM myo-inositol, 2 mM sodium pyruvate, 25 mM $NaHCO_3$, 25 mM glucose, and bubbled with 5% CO_2/95% O_2. For recording mEPSCs, the ACSF contained 0.5 μM strychnine and 10 μM SR95531, 50 μM D(−)-2-amino-5-phosphonovaleric acid and 0.5 μM TTX. Slices were viewed using Dodt contrast optics and a 40× water immersion lens, and recordings made using an Axon Multiclamp 700B amplifier (Molecular Devices). The postsynaptic recording pipette solution contained 110 mM $CsCH_3SO_3$, 5 mM CsCl, 1 mM $MgCl_2$, 4 mM MgATP, 0.4 mM TrisGTP, 14 mM Tris-phosphocreatine, 5 mM EGTA and 10 mM HEPES, adjusted to pH 7.30 with CsOH (290 mOsm). The K^+-based solution in the presynaptic electrodes contained 110 mM KCH_3SO_3, 20 mM KCl, 4 mM MgATP, 0.3 mM Tris-GTP, 5 mM sodium phosphocreatine, 9 mM $Tris_2$-phosphocreatine, 0.2 mM EGTA, 10 mM HEPES and 1 mM glutamate, adjusted to pH 7.30 with KOH. The K^+-free presynaptic solution contained 110 mM NMDG-CH_3SO_3, 20 mM NMDG-Cl, 4 mM MgATP, 0.3 mM Tris-GTP, 5 mM sodium phosphocreatine, 9 mM $Tris_2$-phosphocreatine, 0.2 mM EGTA, 10 mM HEPES and 1 mM glutamate, adjusted to pH 7.30 with NMDG. The low Na^+ and K^+-free presynaptic solution contained 110 mM NMDG-CH_3SO_3, 20 mM NMDG-Cl, 4 mM Mg-ATP, 0.3 mM Na_3-GTP, 10 mM $Tris_2$-phosphocreatine, 0.2 mM EGTA, 10 mM HEPES and 1 mM glutamate, adjusted to pH 7.30 with NMDG. In some experiments, 20 μM Alexa-594 was also added to the presynaptic solution. Calyces were clamped at −80 mV (for K^+-based solution, corrected for junction potential of 10 mV) or −75 mV (for NMDG-based solution, corrected for a 5-mV junction potential). Postsynaptic cells were clamped at −82 mV (including junction potential of 12 mV). Two tests were used to confirm recording from a calyx. First, the fluorescent dye fill of the calyx was visualized at the end of each recording. Second, a depolarizing voltage was injected into the calyx and increased mEPSC frequency or a large postsynaptic response was measured. Signals were filtered at 10 kHz and sampled at 20 kHz. During recordings with NMDG or EIPA, the mEPSC frequency dropped to a variable extent. For example, in the 10 mM Na^+ condition, these changes were, for K^+, 7.7 ± 3.2 Hz (range, 2.4–16.9) at 0–2 min and 6.8 ± 0.5 Hz (range, 5.7–7.8) at 25–30 min (P = 0.76, paired t test); for $NMDG^+$, 8.2 ± 2.4 Hz (range, 1.1–15.9) at 0–2 min and 2.7 ± 1.6 Hz (range, 0.4–8.8) at 25–30 min (P = 0.015, paired t test); and for EIPA, 13.2 ± 2.9 Hz (range, 5.1–18.6) at 0–2 min and 2.6 ± 0.8 Hz (range, 0.7–4.8) at 25–30 min (P = 0.017, paired t test). These changes might reflect, at least in part, detection problems as mEPSC amplitude dropped, but this possibility was not explored further.

Data analysis. mEPSCs were detected using a sliding template algorithm[49], with a rise time of 0.2 ms and decay of 0.5 ms, threshold of 4× noise s.d., using

Axograph X. Data were analyzed using Clampfit 9.2 (Molecular Devices) and Igor 6.0 (Wavemetrics), and expressed as mean ± s.e.m.

Statistical analysis. All mean data were obtained from at least three measurements using at least two different synaptic vesicle preparations. Statistical significance was assessed by two-tailed paired *t* tests, unless otherwise indicated.

47. Hell, J.W. & Jahn, R. eds. *Preparation of Synaptic Vesicles from Mammalian Brain* (Academic Press, San Diego, 1994).
48. Borst, J.G., Helmchen, F. & Sakmann, B. Pre- and postsynaptic whole-cell recordings in the medial nucleus of the trapezoid body of the rat. *J. Physiol. (Lond.)* **489**, 825–840 (1995).
49. Huang, H. & Trussell, L.O. Control of presynaptic function by a persistent Na^+ current. *Neuron* **60**, 975–979 (2008).

doi:10.1038/nn.2898

Corrigendum: Presynaptic regulation of quantal size: K^+/H^+ exchange stimulates vesicular glutamate transport

Germaine Y Goh, Hai Huang, Julie Ullman, Lars Borre, Thomas S Hnasko, Laurence O Trussell & Robert H Edwards
***Nat. Neurosci.* 14, 1285–1292 (2011); published online 28 August 2011; corrected online 13 October 2011**

In the version of this article initially published online, the composition of the low-sodium and potassium-free NMDG patch clamp solution was omitted and a non-NMDG solution, not used in this work, was given instead. The error has been corrected in the PDF and HTML versions of this article.